

Iron-titanium oxides as an indicator of the role of the fluid phase during the cooling of granites metamorphosed to granulite grade

HUGH R. ROLLINSON

Department of Earth Sciences, The University, Leeds LS2 9JT

SUMMARY. A detailed electron probe study of iron-titanium oxide intergrowths from slowly cooled granitic rocks from the granulite grade, Archaean Scourian complex of north-west Scotland has yielded a wealth of information about magmatic and metamorphic temperatures, subsolidus cooling, and the behaviour of the fluid phase during cooling. Five stages are documented in the cooling history of granites and trondhjemites which include: (i) magmatic-subsolidus cooling (1035 °C–890 °C); (ii) granulite facies metamorphism and the accompanied expulsion of a hydrous fluid phase (890 °C–830 °C); (iii) subsolidus cooling following the peak of the granulite facies metamorphism (830 °C–660 °C); (iv) the localized reintroduction of water into the rocks during retrogression (660 °C–530 °C) and (v) subsolidus cooling and re-equilibration in the presence of a finite amount of H₂O (530 °C–320 °C).

THE detailed study of iron-titanium oxide intergrowths from slowly cooled rocks can yield a wealth of information about the magmatic and metamorphic temperatures and the subsequent subsolidus cooling history of a rock (Anderson, 1968; Duchesne, 1972; Bowles, 1976, 1977; Oliver, 1978; Rollinson, 1979). The purpose of this study is to show that in addition to the cooling history it is possible, from a study of iron-titanium oxides, to monitor the behaviour of the fluid phase during the cooling of plutonic rocks.

Detailed electron-probe analyses were made on ten composite ilmenite-magnetite grains from three granite sheets from the granulite grade Scourian complex, north-west Scotland. The samples were collected from the area between Scourie and Badcall, Sutherland, where granitic (s.s.) rocks form a minor part of the Archaean granulite facies gneisses; they form sheets 2–3 m wide and a few hundred metres long, intrusive into tonalitic gneiss and gabbro. The granites represent the last stages of a tonalite-trondhjemite-granite suite (Rollinson and Windley, in prep.) which was subsequently metamorphosed to granulite grade. A

relict graphic texture is sometimes found, but more commonly deformation has given rise to flattened lenticles of quartz and ferromagnesian minerals. A typical mineralogy is bluish quartz, plagioclase, mesoperthite, orthopyroxene, or almandine garnet with or without iron-titanium oxides. Samples, 67, 68, and 69 come from the same granite sheet on the Shios peninsula (NC 138447) and sample 82 from a separate granite sheet a few metres to the east; sample 35 was collected on Torran nan Clach Boga (NC 157425), north of Upper Badcall. The feldspars in these rocks have also been analysed and are the subject of a separate study (Rollinson, in prep.).

Iron-titanium oxides from Scourian granites form intergrowths of ilmenite and magnetite which show either high temperatures (660 °C–910 °C) or low equilibration temperatures (530 °C–320 °C) on the Buddington and Lindsley (1964) thermometer (fig. 2). High-temperature grains are composed of about equal proportions of ilmenite and magnetite and form simple bipartite grains; there may be fine lamellae of ilmenite in a magnetite host and more rarely fine lamellae of magnetite in ilmenite. Low temperature grains form simple bipartite intergrowths or contain lamellae of magnetite 10 to 60 μm wide in a host of ilmenite; in low-temperature grains ilmenite dominates over magnetite (fig. 1).

Analytical procedure. A detailed description of the electron-probe method used is given in Rollinson (1979); in addition to the standards quoted, natural rutile (59.69% Ti, 0.33% Fe, 39.98% O) was used to determine Ti, and synthetic wollastonite (23.58% Si, 34.52% Ca, 41.59% O) for Ca and Si. Both a scanning beam and a point (less than 1 μm diameter) were used to analyse areas of grains and domains within grains respectively. It will be noted that the totals for magnetite analyses are low. They are lower in the high-temperature than the low-temperature grains suggesting that magnetite is not stoichiometric due to late alteration to γ-maghemite. Grains which continued

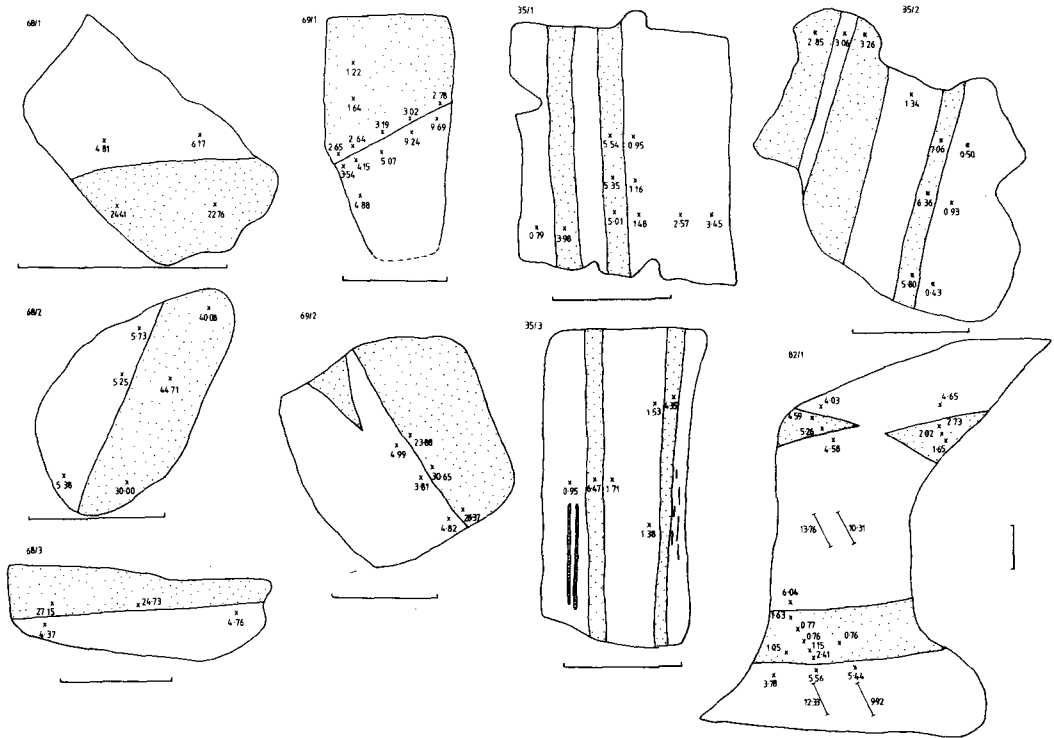


FIG. 1. Iron-titanium oxide grains analysed in this study; stippled areas are magnetite, unshaded areas are ilmenite. The mole % ulvöspinel in magnetite and R_2O_3 in ilmenite are shown. Grains 68/1, 68/2, 68/3, and 69/2 yield high-equilibration temperatures, and grains 69/1, 35/1, 35/2, 35/3, and 82/1 yield low-equilibration temperatures. The scale bar is 50 microns.

to equilibrate with ilmenite to low temperatures are less susceptible to this form of late alteration. Values for FeO and Fe_2O_3 , mol per cent ulvöspinel and mole per cent R_2O_3 ($Fe_2O_3 + Al_2O_3 + Cr_2O_3$) were calculated using the method of Carmichael (1967).

Scanning analyses were made over areas containing fine lamellae in the high-temperature grains in order to estimate the pre-exsolution composition of the grain. These are termed 'average grains' in Table I. Point analyses were made 5 to 10 μm away from the boundary separating ilmenite and magnetite lamellae in several places in the same grain along the length of the lamellae and also normal to the length of lamellae in order to check for compositional zoning. The analysed grains and the mole fraction of ulvöspinel and R_2O_3 in ilmenite and magnetite respectively are depicted in fig. 1. Adjacent ilmenite-magnetite point analyses are used to estimate the equilibration temperature at that particular point in the grain from the Buddington and Lindsley thermometer. This assumes that whilst grains are zoned with respect to their mole fraction of ulvöspinel and R_2O_3 equilibrium is preserved in small microsystems within the grain and that, if oxygen is lost or gained in the system, iron and titanium will move between ilmenite and magnetite as a response. This means that a variety of equilibration temperatures

may be obtained for a single grain and that limits can be set on the distance over which iron and titanium can diffuse at the temperature in question.

The experiments of Buddington and Lindsley (1964) were carried out in the pure system $FeO-Fe_2O_3-TiO_2$, so that any impurities in natural iron-titanium oxides involve a certain amount of extrapolation in order to estimate temperature and oxygen fugacity at equilibrium. Powell and Powell (1977) developed a method which estimates the effect of minor elements on the activities of the magnetite, ulvöspinel, hematite, and ilmenite components; since, however, it is not clear what components the minor elements make within the rhombohedral and spinel phases it is only possible to set limits on the activities of magnetite, ilmenite, ulvöspinel, and hematite. The activities of the phases are combined to give the most and least favourable alternatives which are then used with the experimental data of Buddington and Lindsley (1964) to give a maximum and minimum temperature and oxygen fugacity. The results are plotted with their estimated uncertainty in fig. 2. The only drawback with this method is that the mineral analysis has to be calculated to three and four oxygens for ilmenite and magnetite respectively, which for microprobe analyses involves some assumptions, since the calculation of Fe^{3+} depends

IRON-TITANIUM OXIDES

TABLE 1. Co-existing ilmenite and magnetite in samples BR 67, 68, 69 from the Shies peninsula

| Rock/Grain Anal. No. | ILMENITE | | | | | | | | | | MAGNETITE | | | | | | | | | | | | | | | | | | | | | | | |
|--------------------------------|-----------------|----------|-----------|---------|---------|----------------------|---------|-------|--------|--------|------------------------|---------|--------|---------|--------|-----------------|--------|--------|--------|--------|----------------------|--------|--------|--------|--------|------------------------|--------|--------|--------|--------|--------|--------|--------|--------|
| | Averaged grains | | | | | Grain-boundary pairs | | | | | Low temperature grains | | | | | Averaged grains | | | | | Grain-boundary pairs | | | | | Low temperature grains | | | | | | | | |
| | 1 | 2 | 3 | 4 | 5 | 6 | 7 | 8 | 9 | 10 | 11 | 12 | 13 | 14 | 15 | 16 | 17 | 18 | 19 | 20 | 21 | 22 | 23 | 24 | 25 | 26 | 27 | 28 | 29 | 30 | 31 | 32 | 33 | 34 |
| SiO ₂ | 68/3 | 68/2 | 69/2 | 68/2 | 68/2 | 67/1 | 68/2 | 69/2 | 69/2 | 69/2 | 68/1 | 68/3 | 68/1 | 68/3 | 69/1 | 69/1 | 69/1 | 69/1 | 69/1 | 69/1 | 69/1 | 69/1 | 69/1 | 69/1 | 69/1 | 69/1 | 69/1 | 69/1 | 69/1 | 69/1 | 69/1 | 69/1 | 69/1 | 69/1 |
| TiO ₂ | 1152/16 | 1145/7,8 | 973/1,2,3 | 1145/14 | 1145/15 | 948/6 | 1145/5 | 973/6 | 973/9 | 973/12 | 1145/3 | 1152/15 | 1145/4 | 1152/17 | 972/19 | 972/21 | 972/24 | 972/24 | 972/24 | 972/21 | 972/21 | 972/21 | 972/21 | 972/21 | 972/21 | 972/21 | 972/21 | 972/21 | 972/21 | 972/21 | 972/21 | 972/21 | 972/21 | 972/21 |
| Al ₂ O ₃ | 0.14 | 0.20 | - | 0.14 | 0.12 | 0.06 | 0.17 | - | - | - | 0.14 | 0.15 | 0.14 | 0.15 | 0.15 | - | - | - | - | - | - | - | - | - | - | - | - | - | - | - | - | - | - | - |
| FeO | 46.29 | 47.56 | 49.83 | 49.34 | 49.40 | 47.77 | 49.15 | 49.27 | 49.89 | 49.55 | 48.46 | 50.04 | 49.59 | 49.63 | 46.63 | 47.11 | 48.86 | 49.99 | 49.33 | 46.63 | 47.11 | 48.86 | 49.99 | 49.33 | 46.63 | 47.11 | 48.86 | 49.99 | 49.33 | 46.63 | 47.11 | 48.86 | 49.99 | 49.33 |
| Fe ₂ O ₃ | 0.08 | 0.06 | 0.06 | 0.05 | 0.03 | 0.05 | 0.08 | 0.04 | 0.03 | 0.03 | 0.03 | 0.03 | 0.03 | 0.03 | 0.03 | 0.03 | 0.04 | 0.03 | 0.03 | 0.03 | 0.03 | 0.03 | 0.03 | 0.03 | 0.03 | 0.03 | 0.03 | 0.03 | 0.03 | 0.03 | 0.03 | 0.03 | 0.03 | 0.03 |
| FeO* | 50.91 | 48.80 | 41.83 | 48.91 | 49.28 | 41.70 | 48.80 | 41.91 | 41.87 | 42.72 | 49.01 | 48.36 | 48.88 | 48.40 | 42.35 | 42.92 | 40.32 | 40.32 | 39.09 | 42.35 | 42.92 | 40.32 | 40.32 | 40.32 | 42.35 | 42.92 | 40.32 | 40.32 | 40.32 | 42.35 | 42.92 | 40.32 | 40.32 | 40.32 |
| MnO | 0.72 | 0.25 | 6.75 | 0.24 | 0.27 | 5.74 | 0.23 | 6.67 | 6.37 | 6.29 | 0.31 | 0.72 | 0.31 | 0.72 | 7.94 | 8.30 | 8.11 | 8.36 | 8.34 | 7.94 | 8.30 | 8.11 | 8.36 | 8.34 | 7.94 | 8.30 | 8.11 | 8.36 | 8.34 | 7.94 | 8.30 | 8.11 | 8.36 | 8.34 |
| MgO | 0.08 | 0.15 | 0.05 | 0.19 | 0.20 | 0.00 | 0.17 | 0.04 | 0.03 | 0.06 | 0.05 | 0.06 | 0.05 | 0.02 | 0.03 | 0.03 | 0.02 | 0.02 | 0.02 | 0.03 | 0.03 | 0.03 | 0.02 | 0.02 | 0.03 | 0.03 | 0.02 | 0.02 | 0.02 | 0.03 | 0.03 | 0.02 | 0.02 | 0.02 |
| CaO | 0.00 | 0.01 | - | 0.00 | 0.00 | 0.05 | 0.00 | - | - | - | 0.00 | 0.01 | 0.00 | 0.01 | 0.01 | - | - | - | - | - | - | - | - | - | - | - | - | - | - | - | - | - | - | - |
| TOTAL | 98.25 | 97.05 | 98.07 | 98.79 | 98.73 | 98.65 | 98.65 | 97.93 | 98.98 | 98.66 | 98.04 | 99.11 | 99.06 | 99.03 | 98.86 | 98.41 | 97.76 | 98.06 | 98.03 | 98.86 | 98.41 | 97.76 | 98.06 | 98.03 | 98.86 | 98.41 | 97.76 | 98.06 | 98.03 | 98.86 | 98.41 | 97.76 | 98.06 | 98.03 |
| FeO | 40.92 | 42.48 | 37.88 | 43.85 | 43.94 | 37.15 | 43.87 | 37.48 | 38.36 | 38.08 | 43.34 | 44.41 | 43.98 | 44.41 | 33.84 | 33.90 | 35.69 | 36.41 | 35.88 | 33.84 | 33.90 | 35.69 | 36.41 | 35.88 | 33.84 | 33.90 | 35.69 | 36.41 | 35.88 | 33.84 | 33.90 | 35.69 | 36.41 | 35.88 |
| Fe ₂ O ₃ | 11.10 | 8.41 | 4.39 | 5.40 | 5.94 | 5.06 | 5.46 | 4.92 | 3.90 | 5.16 | 6.30 | 4.48 | 4.97 | 4.91 | 9.46 | 10.02 | 5.15 | 4.28 | 3.57 | 9.46 | 10.02 | 5.15 | 4.28 | 3.57 | 9.46 | 10.02 | 5.15 | 4.28 | 3.57 | 9.46 | 10.02 | 5.15 | 4.28 | 3.57 |
| TOTAL | 95.37 | 99.12 | 96.96 | 99.32 | 99.92 | 95.88 | 99.15 | 98.22 | 96.60 | 99.17 | 98.67 | 99.88 | 99.51 | 99.52 | 97.92 | 97.87 | 97.87 | 99.12 | 97.17 | 97.92 | 97.87 | 99.12 | 97.87 | 97.17 | 97.92 | 97.87 | 99.12 | 97.87 | 97.17 | 97.92 | 97.87 | 99.12 | 97.87 | 97.17 |
| R ₂ O ₃ | 10.82 | 8.19 | 4.30 | 5.25 | 5.73 | 5.09 | 5.36 | 4.82 | 3.81 | 4.99 | 6.17 | 4.37 | 4.81 | 4.76 | 9.24 | 9.69 | 5.07 | 4.15 | 3.54 | 9.24 | 9.69 | 5.07 | 4.15 | 3.54 | 9.24 | 9.69 | 5.07 | 4.15 | 3.54 | 9.24 | 9.69 | 5.07 | 4.15 | 3.54 |
| SiO ₂ | 1152/13 | 1145/5,6 | 973/4,5,6 | 1145/13 | 1145/16 | 848/7 | 1145/10 | 973/7 | 973/10 | 973/11 | 1145/2 | 1152/14 | 1145/1 | 1152/18 | 972/20 | 972/22 | 972/23 | 972/23 | 972/25 | 972/20 | 972/22 | 972/23 | 972/23 | 972/25 | 972/20 | 972/22 | 972/23 | 972/23 | 972/25 | 972/20 | 972/22 | 972/23 | 972/23 | 972/25 |
| TiO ₂ | 0.15 | 0.14 | - | 0.11 | 0.16 | 0.12 | 0.16 | - | - | - | 0.17 | 0.16 | 0.16 | 0.14 | - | - | - | - | - | - | - | - | - | - | - | - | - | - | - | - | - | - | - | - |
| Al ₂ O ₃ | 14.73 | 14.63 | 15.77 | 14.81 | 13.20 | 9.28 | 9.80 | 9.30 | 10.07 | 7.84 | 7.31 | 8.82 | 7.88 | 8.02 | 1.02 | 1.02 | 1.07 | 0.89 | 0.89 | 1.02 | 1.02 | 1.07 | 0.89 | 0.89 | 1.02 | 1.02 | 1.07 | 0.89 | 0.89 | 1.02 | 1.02 | 1.07 | 0.89 | 0.89 |
| FeO | 0.13 | 0.30 | 0.12 | 0.13 | 0.17 | 0.16 | 0.15 | 0.16 | 0.15 | 0.15 | 0.12 | 0.16 | 0.14 | 0.12 | 0.23 | 0.27 | 0.24 | 0.25 | 0.24 | 0.23 | 0.27 | 0.24 | 0.25 | 0.24 | 0.23 | 0.27 | 0.24 | 0.25 | 0.24 | 0.23 | 0.27 | 0.24 | 0.25 | 0.24 |
| Fe ₂ O ₃ | 0.08 | 0.10 | 0.07 | 0.11 | 0.10 | 0.05 | 0.11 | 0.09 | 0.07 | 0.09 | 0.04 | 0.09 | 0.07 | 0.11 | 0.07 | 0.04 | 0.06 | 0.06 | 0.06 | 0.07 | 0.04 | 0.06 | 0.06 | 0.06 | 0.07 | 0.04 | 0.06 | 0.06 | 0.06 | 0.07 | 0.04 | 0.06 | 0.06 | 0.06 |
| FeO* | 76.01 | 76.40 | 71.66 | 76.49 | 77.64 | 79.61 | 80.69 | 79.37 | 79.05 | 80.85 | 82.23 | 81.27 | 81.88 | 81.76 | 89.75 | 89.75 | 89.80 | 89.12 | 89.10 | 89.75 | 89.80 | 89.12 | 89.57 | 89.10 | 89.75 | 89.80 | 89.12 | 89.57 | 89.10 | 89.75 | 89.80 | 89.12 | 89.57 | 89.10 |
| MnO | 0.14 | 0.06 | 1.40 | 0.02 | 0.10 | 0.26 | 0.04 | 0.22 | 0.22 | 0.34 | 0.08 | 0.14 | 0.02 | 0.04 | 0.07 | 0.10 | 0.06 | 0.12 | 0.10 | 0.07 | 0.10 | 0.06 | 0.12 | 0.10 | 0.07 | 0.10 | 0.06 | 0.12 | 0.10 | 0.07 | 0.10 | 0.06 | 0.12 | 0.10 |
| MgO | 0.00 | 0.06 | 0.03 | 0.00 | 0.08 | 0.00 | 0.00 | 0.09 | 0.02 | 0.01 | 0.00 | 0.00 | 0.00 | 0.01 | 0.02 | 0.03 | 0.01 | 0.02 | 0.06 | 0.02 | 0.03 | 0.01 | 0.02 | 0.06 | 0.02 | 0.03 | 0.01 | 0.02 | 0.06 | 0.02 | 0.03 | 0.01 | 0.02 | 0.06 |
| CaO | 0.02 | 0.01 | - | 0.00 | 0.00 | 0.02 | 0.00 | - | - | - | 0.02 | 0.01 | 0.01 | 0.03 | - | - | - | - | - | - | - | - | - | - | - | - | - | - | - | - | - | - | - | - |
| TOTAL | 91.25 | 91.70 | 90.05 | 91.66 | 91.46 | 90.95 | 90.95 | 90.22 | 90.59 | 90.26 | 90.66 | 90.16 | 90.16 | 90.34 | 91.17 | 91.16 | 90.95 | 90.95 | 90.36 | 91.17 | 91.16 | 90.95 | 90.95 | 90.36 | 91.17 | 91.16 | 90.95 | 90.95 | 90.36 | 91.17 | 91.16 | 90.95 | 90.95 | 90.36 |
| FeO | 41.21 | 41.28 | 31.85 | 43.51 | 41.91 | 37.75 | 38.98 | 37.46 | 38.34 | 36.21 | 36.44 | 37.93 | 37.06 | 37.12 | 31.20 | 31.10 | 31.07 | 30.69 | 30.76 | 31.20 | 31.10 | 31.07 | 30.69 | 30.76 | 31.20 | 31.10 | 31.07 | 30.69 | 30.76 | 31.20 | 31.10 | 31.07 | 30.69 | 30.76 |
| Fe ₂ O ₃ | 36.45 | 36.81 | 42.21 | 36.65 | 39.71 | 46.52 | 46.15 | 46.58 | 45.24 | 49.61 | 50.88 | 48.17 | 49.81 | 49.61 | 65.07 | 65.24 | 64.51 | 65.14 | 64.84 | 65.07 | 65.24 | 64.51 | 65.14 | 64.84 | 65.07 | 65.24 | 64.51 | 65.14 | 64.84 | 65.07 | 65.24 | 64.51 | 65.14 | 64.84 |
| TOTAL | 91.91 | 95.37 | 91.47 | 95.34 | 94.16 | 95.55 | 94.11 | 91.90 | 94.11 | 94.25 | 95.07 | 95.30 | 95.15 | 95.20 | 97.66 | 97.72 | 97.05 | 97.44 | 96.95 | 97.66 | 97.72 | 97.05 | 97.44 | 96.95 | 97.66 | 97.72 | 97.05 | 97.44 | 96.95 | 97.66 | 97.72 | 97.05 | 97.44 | 96.95 |
| Imp | 44.82 | 44.20 | 48.05 | 44.71 | 40.08 | 28.72 | 30.00 | 28.37 | 30.65 | 23.88 | 22.76 | 27.15 | 24.41 | 24.73 | 3.02 | 2.78 | 3.19 | 2.64 | 2.65 | 3.02 | 2.78 | 3.19 | 2.64 | 2.65 | 3.02 | 2.78 | 3.19 | 2.64 | 2.65 | 3.02 | 2.78 | 3.19 | 2.64 | 2.65 |
| Thak | 910 | 829 | 828 | 787 | 775 | 707 | 707 | 707 | 691 | 684 | 680 | 667 | 662 | 664 | 533 | 530 | 487 | 457 | 449 | 533 | 530 | 487 | 457 | 449 | 533 | 530 | 487 | 457 | 449 | 533 | 530 | 487 | 457 | 449 |
| Tmin | 906 | 825 | 804 | 785 | 771 | 706 | 705 | 701 | 687 | 678 | 678 | 663 | 661 | 662 | 527 | 522 | 483 | 450 | 445 | 527 | 522 | 483 | 450 | 445 | 527 | 522 | 483 | 450 | 445 | 527 | 522 | 483 | 450 | 445 |
| -f _{0,gran} | 11.6 | 13.8 | 14.3 | 15.2 | 15.2 | 16.8 | 16.8 | 17.0 | 17.8 | 17.7 | 17.0 | 18.1 | 18.0 | 18.0 | 19.4 | 19.4 | 22.3 | 23.7 | 24.3 | 19.4 | 19.4 | 22.3 | 23.7 | 24.3 | 19.4 | 19.4 | 22.3 | 23.7 | 24.3 | 19.4 | 19.4 | 22.3 | 23.7 | 24.3 |
| -f _{0,min} | 11.7 | 13.9 | 15.3 | 15.2 | 15.4 | 17.1 | 16.9 | 17.3 | 18.1 | 17.4 | 17.2 | 18.3 | 18.1 | 18.1 | 19.9 | 20.0 | 22.7 | 24.5 | 24.9 | 19.9 | 20.0 | 22.7 | 24.5 | 24.9 | 19.9 | 20.0 | 22.7 | 24.5 | 24.9 | 19.9 | 20.0 | 22.7 | 24.5 | 24.9 |

FeO total iron determined as FeO

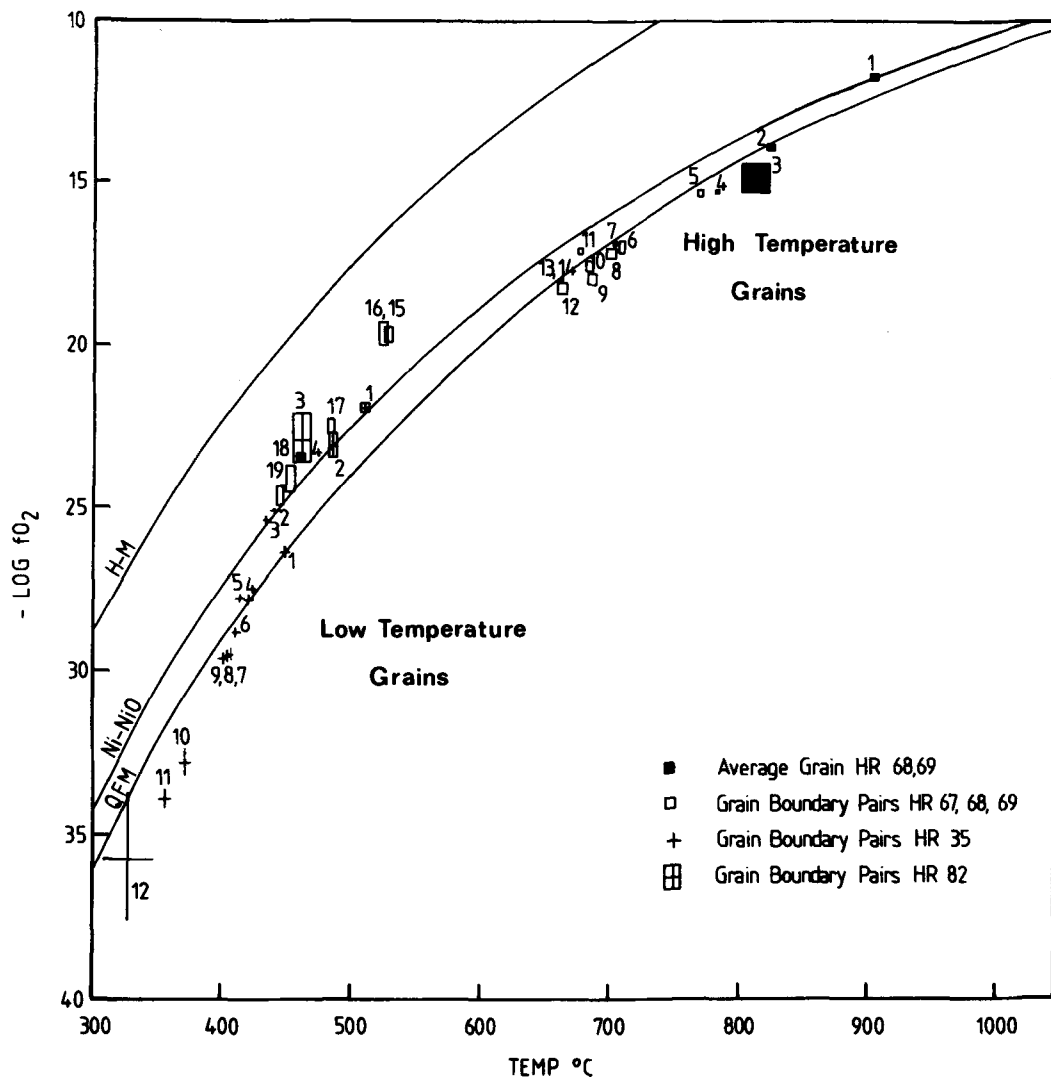


FIG. 2. Oxygen fugacity-temperature curves for iron-titanium oxide pairs from Scourian granites. Error bars are from the method of Powell and Powell (1977); buffer curves are calculated for 8 kb total pressure after Eugster and Wones (1962). Sample numbers refer to analyses in tables 1 to 3. H-M hematite-magnetite buffer; Ni-NiO nickel-nickel oxide buffer; QFM quartz-fayalite-magnetite buffer.

upon the way in which the minor elements are treated. Manganese in ilmenite is the only minor element of importance and occurs up to 8.6 wt% MnO in grain 69/1, but since the spinel phase is almost pure magnetite-ulvöspinel solid solution, the uncertainty is small.

Ilmenite-magnetite chemistry. The variation in composition across grains is shown in fig. 1. Whilst there is variation in the mole per cent of ulvöspinel in the high-temperature grains (44-23 mole %), the only evidence of zoning is in grain 68/2 in which the mole fraction of ulvöspinel decreases towards

the edge of the grain. Low-temperature grains show strong zoning:

(i) *a.* Magnetite increases in mole % ulvöspinel towards ilmenite (grains 69/1, 82/1); *b.* magnetite is richer in mole % ulvöspinel in an ilmenite-rich environment than in an ilmenite-poor environment (grain 35/2).

(ii) Magnetite decreases in mole % ulvöspinel along the length of a lamella towards the edge of a grain (grain 35/1) and even parallel to an ilmenite-magnetite boundary (grain 69/1).

(iii) Ilmenite increases in mole % R_2O_3 away from magnetite (grains 69/1, 35/1).

(iv) Ilmenite increases in mole % R_2O_3 towards the edge of a grain even when parallel to a magnetite lamella (grains 82/1, 35/2, 35/3) although in grain 69/1 R_2O_3 increases across the grain.

(v) Manganese in ilmenite increases towards the edge of a grain in both high- and low-temperature grains (grains 69/1, 69/2, 82/1) although in the lowest temperature grains this is reversed and Mn decreases towards the edge of the grain (grain 35/1).

Manganese is variable in ilmenite from 0.2 to 6.7 weight % in high-temperature grains and from 1.9 to 8.6 wt % in low-temperature grains. This is not related to the composition of the host rock, as samples 69 and 82 contain the same amount of MnO (0.03–0.04 wt % MnO) and yet ilmenite grains contain twice as much MnO in sample 69 as in sample 82. Also the variation of MnO in ilmenite within a single granite sheet 0.2–0.8% MnO in sample 68 and 8.6% MnO in sample 69 suggests that it is as a result of local exchange reactions (probably with orthopyroxene) rather than an original feature of the rock.

Electron-probe scans across and X-ray images of grain 82/1 show that cracks in magnetite are enriched in MgO (c. 17.0%); these cracks also contain Al_2O_3 (c. 11.0%) and minimal Cr, Fe, and Ti. Bowles (1976) reported fine lamellae of ceylonite associated with magnetite in ilmenite–magnetite intergrowths in the gabbros of the Freetown Complex, Sierra Leone, and it may be that this is an alteration product of this or spinel associated with magnetite.

Thermometry and cooling history. A plot of equilibration temperature versus oxygen fugacity as determined from the experimental data of Buddington and Lindsley (1964) using the method of Powell and Powell (1977) for iron–titanium oxides in Scourian granites shows two distinct cooling curves (fig. 2). These data are combined with high-temperature oxide data from cogenetic trondhjemites from the same area, described in an earlier study (Rollinson, 1979); the trondhjemite analyses were recalculated using the method of Powell and Powell (1977) in order to estimate the uncertainty of the position in fO_2 – T space (fig. 3). The combined iron–titanium oxide cooling curve for the trondhjemite–granite suite at Scourie has three distinct sections (fig. 3), marked by changes in oxygen fugacity relative to standard buffer curves, calculated for 8 kb total pressure (after Eugster and Wones, 1962): (i) a high-temperature section (1035 °C–890 °C, defined predominantly by the trondhjemite samples but including one granite

sample, with the oxygen fugacity buffered just above the Ni–NiO buffer curve; (ii) an intermediate-temperature section 830 °C–660 °C defined by the ‘high-temperature’ grains described above, with the oxygen fugacity buffered parallel to the QFM buffer curve; and (iii) a low temperature section (530 °C–320 °C) defined by the ‘low-temperature’ grains described above, with the oxygen fugacity unbuffered. There is a small decrease in the oxygen fugacity of about one log unit, relative to the buffer curves, between the high and intermediate temperature sections and a large increase in oxygen fugacity between the intermediate- and low-temperature sections on the curve (fig. 3).

The highest temperatures in the trondhjemites (1035 °C) and in the granites (910 °C) are consistent with magmatic temperatures in relatively dry melts (Whitney, 1975; Wyllie, 1977) and the high-temperature section of the curve is therefore interpreted as magmatic–subsolvus cooling. The change in oxygen fugacity between the high and intermediate sections of the cooling curve falls in the temperature range 890 °C–830 °C, which coincides with temperatures calculated for peak of the granulite facies metamorphism in the Scourian complex. Garnet–pyroxene equilibria suggest that the peak of the granulite facies metamorphism was at 820 °C on the Scottish mainland (Rollinson, 1978), and in the range 800 °C–860 °C in South Harris (Wood, 1975, 1977); plagioclase–scapolite equilibria suggest slightly higher temperatures for the Scottish mainland (c. 915 °C) although there is a larger uncertainty on this temperature estimate (Rollinson, in press).

The principal control of oxygen fugacity in the Scourie granites and trondhjemites is the dissociation of H_2O and CO_2 , which in turn is a function of the absolute amount of the fluid phase present and the H_2O – CO_2 ratio. For example, the equilibrium constant K for the dissociation of H_2O is given by:

$$K = \frac{f(H_2O)}{f(H_2) \cdot f(O_2)^{\frac{1}{2}}}$$

Since K is a constant dependent only upon temperature (Eugster, 1977) a decrease in the activity of H_2O at a given temperature will be associated with a decrease in the activity of O_2 . It is proposed that the reduction in oxygen fugacity in the temperature interval 890 °C–830 °C is related to a change in the nature of the fluid phase due to the onset of the granulite-facies metamorphism. There is evidence from trace-element studies (Rollinson and Windley, in prep.) that the igneous precursors of the Scourie granulites contained amphibole although now they contain pyroxenes; there is also

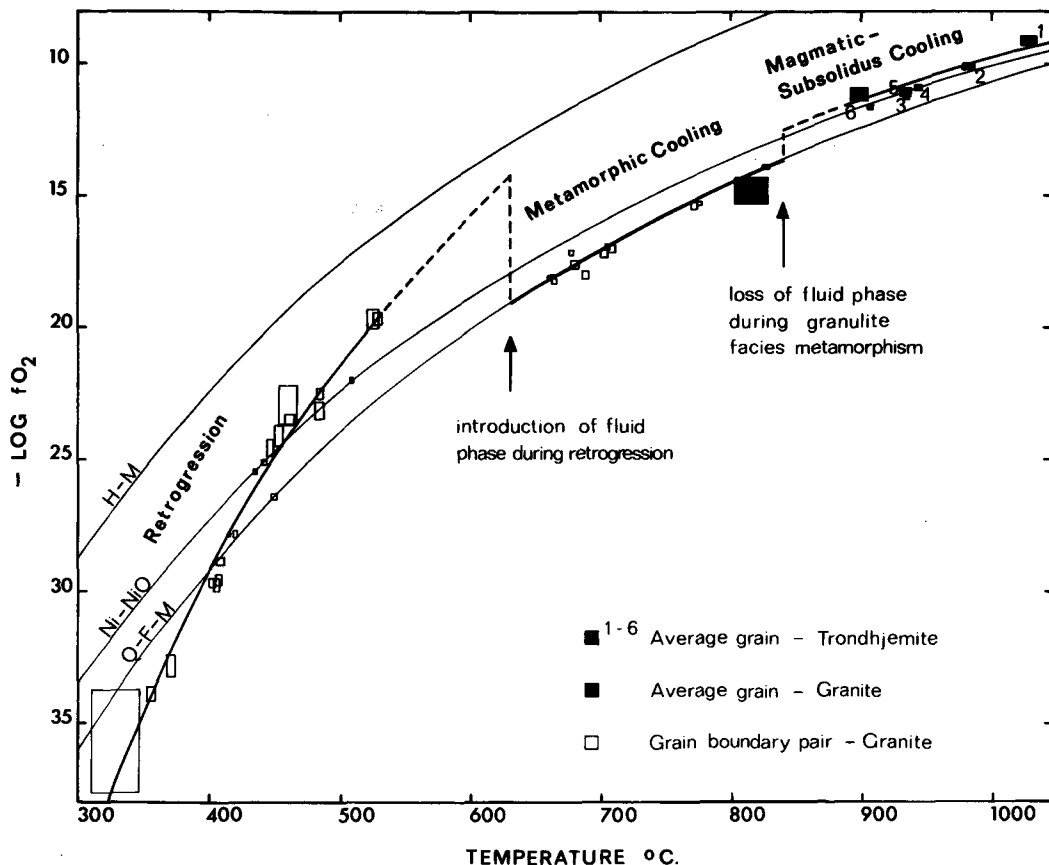


Fig. 3. Oxygen fugacity-temperature curves for iron-titanium oxides from both granites and trondhjemites in the Scourie area. Error bars and oxygen buffers as in fig. 2. The proposed cooling curve, showing changes in oxygen fugacity, is fitted by eye. Data for trondhjemites from Rollinson (1979).

evidence from the feldspars that some granites equilibrated with a melt containing not more than about 3% H_2O (Rollinson, in prep.). It is possible therefore that the recorded change in oxygen fugacity is related to the dehydration of hydrous silicates in the trondhjemite and granite during granulite-facies metamorphism.

The intermediate section of the cooling curve (830 °C–660 °C) represents cooling from the peak of the granulite-facies metamorphism. Oxygen fugacity conditions were buffered parallel to the QFM buffer down to temperatures as low as 660 °C, whereafter there was a sharp increase in oxygen fugacity in the temperature interval 660 °C–530 °C. The increase in oxygen fugacity represents the introduction of a fluid phase into the rock during cooling and accounts for the retrogression of granulite-facies rocks in this area; carbonate is only a minor phase in the Scourian trondhjemites and granites and therefore the fluid phase was

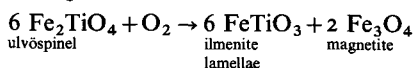
probably predominantly H_2O -rich and contained little CO_2 . The hydrous nature of the fluid phase is further supported by textural evidence from (a) feldspars where water is regarded as the main agent in the extreme coarsening of mesoperthite lamellae, which equilibrated in the temperature range 500 °C–560 °C (Rollinson, in prep.), and (b) orthopyroxenes which are often altered to the hydrous phases biotite and chlorite.

The low-temperature section of the cooling curve cuts across oxygen buffer curves and implies that a finite amount of water was injected into the system and that ilmenite-magnetite pairs re-adjusted their compositions in response to the changing vapour phase and falling temperature, and consumed oxygen in order to regain equilibrium. It is important to bear in mind that the lowest temperature points on fig. 2 involve considerable extrapolation of the Buddington and Lindsley data (1964).

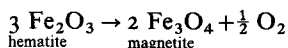
Sample 69 contains both high- and low-temperature oxide grains indicating that the fluid phase can be extremely localized. In general, oxide grains yielding high temperatures are either enclosed in quartz grains or are associated with unaltered quartz aggregates. Low-temperature grains are associated with sericitized feldspar and fine-grained aggregates of quartz.

A dark patch in ilmenite grain 69/1 has the composition FeO 34.57%, TiO₂ 54.24%, MnO 9.2%, Al₂O₃ 0.13%, MgO 0.03%. This grain contains more TiO₂ than can be accommodated in either pure ilmenite or pure ulvöspinel and therefore cannot be expressed as either an ilmenite-hematite solid solution or as an ulvöspinel-magnetite solid solution and is probably a mixture of rutile and magnetite. The ilmenite with which this is associated contains 24% R₂O₃ which is mainly Fe₂O₃. The assemblage Fe₂O₃-ilmenite in the presence of magnetite and rutile yields a minimum temperature of 520 °C at an oxygen fugacity of 10^{-17.5} bars from the hematite-ilmenite solvus of Lindh (1972). This lies on the continuation of the low-temperature curve and is in agreement with the other temperatures and oxygen fugacity conditions determined.

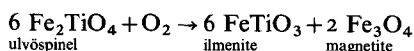
Mechanisms of equilibration. In the high-temperature grains (figs. 1 and 2) the presence of ilmenite lamellae in magnetite indicates that in response to falling temperatures ulvöspinel has reacted to produce ilmenite:



and magnetite lamellae in ilmenite form by the reduction of Fe₂O₃:



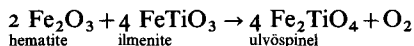
The principal compositional difference between high- and low-temperature grains is the mole % of ulvöspinel in magnetite; in high-temperature grains it is greater than 20% and in low-temperature grains it is 7% or less. In comparison the mole fraction of R₂O₃ in ilmenite is about the same in both high- and low-temperature grains. This suggests that in response to increased oxygen fugacity ulvöspinel reacted to produce ilmenite and magnetite:



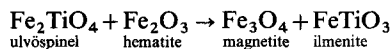
This agrees well with the increased amount of ilmenite in composite ilmenite-magnetite intergrowths in low-temperature grains.

At low temperatures re-equilibration continues on a localized scale to produce zoning as discussed above. The increase in ulvöspinel in magnetite close

to ilmenite and the associated decrease in R₂O₃ in the ilmenite suggests the reaction:



in a restricted zone, which in grain 82/1 is not greater than 15 μm (fig. 1). This is broader than any apparent zonation produced by boundary effects between ilmenite and magnetite. The reduction in R₂O₃ and ulvöspinel towards the edge of a grain may imply some loss of Fe and Ti to silicates, but may also mean that the reaction:



proceeds. This reaction is temperature-sensitive and may imply a gradient across the grain.

Conclusions. The cooling history of plutonic rocks and the behaviour of the fluid phase during cooling can be documented by a detailed study of composite iron-titanium oxides. Five stages are recorded in the cooling history of Scourian granites and trondhjemites: (1) magmatic and subsolidus cooling (1035 °C-890 °C); (2) granulite-facies metamorphism and an accompanied reduction in oxygen activity due to the expulsion of the fluid phase (890 °C-830 °C); (3) subsolidus cooling following granulite facies metamorphism (830 °C-660 °C); (4) localized introduction of a hydrous fluid phase during retrogression, leading to an increase in the oxygen activity (660 °C-530 °C); (5) subsolidus cooling and re-equilibration in the presence of a finite amount of H₂O (530 °C-320 °C).

Several mechanisms are suggested above to explain the variety of oxide temperatures in terms of the continued equilibration between ilmenite and magnetite in a buffered system. A few chemical reactions can be written, which proceeding backwards or forwards on a variety of scales, are sufficient to explain the response of oxide pairs to changing equilibrium conditions. Since oxygen is involved in most of these reactions their 'frozen in' temperature may reflect the availability of oxygen, or more likely hydrogen, since it is more mobile and dependent upon oxygen activity.

Finally it is possible to make some general comments on the implications of the presence of fluids in granulites: (1) The expulsion of a fluid phase during granulite facies metamorphism was proposed by Heier (1973) and Lambert and Heier (1969) to account for the depletion in large ion lithophile elements observed in many high- and intermediate-pressure granulites. This is now independently documented from a study of iron-titanium oxides in the Scourie granulites. (2) Beach and Tarney (1978) proposed that mantle-derived hydrous fluids were responsible for the retrogression of Scourian granulites and that they brought

about a significant redistribution of some major and trace elements. This event may now be constrained to the temperature interval 530 °C–660 °C. (3) The localized introduction of a fluid phase during retrogression has important implications for Sr and Pb isotope systematics in granulites; since some feldspars re-equilibrated during the retrogression (see above) it is likely that Sr and Pb isotopes will be reset or partly reset. Conversely, however, in rocks where retrogression is well established it may be possible to date the 530 °C–660 °C retrogressive event.

Acknowledgements. This study was carried out during the tenure of a Natural Environment Research Council studentship at the University of Leicester. I am grateful to Dr B. F. Windley for his encouragement and advice and to R. N. Wilson for help with the electron-probe analysis. B. F. Windley and J. F. W. Bowles are thanked for their constructive comments on the manuscript.

REFERENCES

- Anderson (A. T.), 1968. *J. Geol.* **76**, 528–47. [M.A. 72-2835]
 Beach (A.) and Tarney (J.), 1978. *Precamb. Res.* **7**, 325–48. [M.A. 79-1444]
 Bowles (J. F. W.), 1976. *Mineral. Mag.* **40**, 703–14 [M.A. 76-3633]
 ——— 1977. *Ibid.* **41**, 103–9. [M.A. 77-2126]
 Buddington (A. F.) and Lindsley (D. H.), 1964. *J. Petrol.* **5**, 310–57. [M.A. 17-278]
 Carmichael (I. S. E.), 1967. *Contrib. Mineral. Petrol.* **14**, 36–64.
 Duchesne (J. C.), 1972. *J. Petrol.* **13**, 57–81. [M.A. 72-2274]
 Eugster (H. P.), 1977. In Fraser, D. G. (ed.), *Thermodynamics in Geology*. D. Reidel, Dordrecht, Holland, pp. 183–202. [M.A. 78-124]
 ——— and Wones (D. R.), 1962. *J. Petrol.* **3**, 82–125. [M.A. 16-526]
 Heier (K. S.), 1973. *Phil. Trans. R. Soc. Lond. A.* **273**, 429–42.
 Lambert (I. B.) and Heier (K. S.), 1969. *Lithos*, **1**, 30–53.
 Lindh (A.), 1972. *Ibid.* **5**, 325–43.
 Oliver (G. J. H.), 1978. *Ibid.* **11**, 147–54.
 Powell (R.) and Powell (M.), 1977. *Mineral. Mag.* **41**, 257–63. [M.A. 77-2886]
 Rollinson (H. R.), 1978. Ph.D. thesis, Univ. Leicester. (Unpubl.)
 ——— 1979. *Mineral. Mag.* **43**, 165–70.
 ——— in press. *Scott. J. Geol.*
 Whitney (J. A.), 1975. *J. Geol.* **83**, 1–31. [M.A. 77-2978]
 Wood (B. J.), 1975. *Earth Planet. Sci. Lett.* **26**, 299–311. [M.A. 77-1163]
 ——— 1977. *Phil. Trans. R. Soc. Lond. A.* **286**, 331–42. [M.A. 77-4243]
 Wyllie (P. J.), 1977. *J. Geol. Soc. Lond.* **134**, 215–34. [M.A. 78-370]
 [Manuscript received 30 August 1979]